ACCOUNTS of chemical research

Article

Cite This: Acc. Chem. Res. 2018, 51, 385−393

pubs.acs.org/accounts

Time-Dependent Density Functional Theory for Open Systems and Its Applications

Shuguang Chen,[‡] YanHo Kwok,[‡] and GuanHua Chen*

Department of Chemistry, the University of Hong Kong, Pofkulam Road, Hong Kong SAR, China

CONSPECTUS: Photovoltaic devices, electrochemical cells, catalysis processes, light emitting diodes, scanning tunneling microscopes, molecular electronics, and related devices have one thing in common: open quantum systems where energy and matter are not conserved. Traditionally quantum chemistry is confined to isolated and closed systems, while quantum dissipation theory studies open quantum systems. The key quantity in quantum dissipation theory is the reduced system density matrix. As the reduced system density matrix is an $O(M! \times M!)$ matrix, where M is the number of the particles of the system of interest, quantum dissipation theory can only be employed to simulate systems of a few particles or degrees of freedom. It is thus important to combine quantum chemistry and quantum dissipation theory so that realistic open quantum systems can be simulated from first-principles.

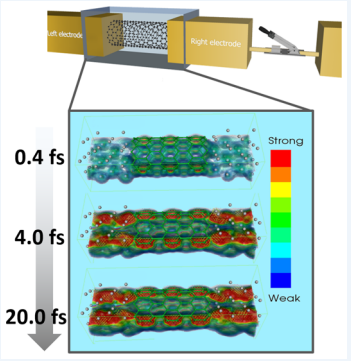

We have developed a first-principles method to simulate the dynamics of open electronic systems, the time-dependent density functional theory for open systems (TDDFT-OS). Instead of the reduced system density matrix, the key quantity is the reduced single-electron density matrix, which is an $N \times N$ matrix where N is the number of the atomic bases of the system of interest. As the dimension of the key quantity is drastically reduced, the TDDFT-OS can thus be used to simulate the dynamics of realistic open electronic systems and efficient numerical algorithms have been developed.

As an application, we apply the method to study how quantum interference develops in a molecular transistor in time domain. We include electron−phonon interaction in our simulation and show that quantum interference in the given system is robust against nuclear vibration not only in the steady state but also in the transient dynamics. As another application, by combining TDDFT-OS with Ehrenfest dynamics, we study current-induced dissociation of water molecules under scanning tunneling microscopy and follow its time dependent dynamics. Given the rapid development in ultrafast experiments with atomic resolution in recent years, time dependent simulation of open electronic systems will be useful to gain insight and understanding of such experiments. This Account will mainly focus on the practical aspects of the TDDFT-OS method, describing the numerical implementation and demonstrating the method with applications.

1. INTRODUCTION

Quantum chemists solve the Schrödinger equation where the number of electrons are conserved and integer.[1] Much has been achieved over the past few decades as computers are ever fast and numeric algorithms are increasingly efficient and accurate. First-principles calculations are now routinely carried out to determine the electronic structures of systems containing hundreds of atoms.[2] With an $O(N)$ algorithm, density-functional theory calculations have been reported to be performed on systems containing millions of atoms.[3,4] With these successes, first-principles methods have been used to study realistic systems and devices beyond simple molecules. On the other hand, in open quantum systems, such as solar cells, light emitting diodes (LEDs), molecular electronic devices, batteries, fuel cells, and photoinduced catalysts, the numbers of electrons are not fixed, are often fractional, and are thus difficult, if not impossible, to model with the conventional quantum chemistry methods.[1,2] The theory of open quantum systems,[5] quantum dissipation theory (QDT), has been well established. Bloch−Redfield theory,[6,7] Lindblad equation,[8] Fokker−Planck equation,[9,10] Feynman−Vermon formalism,[11] Caldeira−Leggett model,[12] and hierarchical equation of motion[13,14] have been developed to investigate open quantum systems and simulate their dynamics. The key quantity in quantum dissipation theory is the reduced density matrix (RDM), which is an $O(M! \times M!)$ matrix, where M is the number of the particles of the system of interest, and in the case of an open electronic system, M is the number of the electrons of the system. To simulate the dynamics of an open quantum system, one needs to solve $O[(M!)^2]$ differential equations. Therefore, traditionally quantum mechanical simulations of open systems are limited to a few particles or to systems of a few energy levels.

The nonequilibrium Green's function (NEGF) formalism has been employed to study quantum transport of molecular electronic devices.[15,16] First-principles NEGF method has been routinely employed to evaluate the steady state currents through electronic devices. However, the dynamic processes of open electronic systems had not been simulated from first-principles until recently.[17] The key quantity in NEGF is the single-electron Green's function $G(\vec{r}, t, \vec{r}', t')$. Time-dependent

Received: August 8, 2017
Published: January 19, 2018

DOI: 10.1021/acs.accounts.7b00382
Acc. Chem. Res. 2018, 51, 385−393

density-functional theory (TDDFT) is used to calculate the excited state properties of electronic systems,[18] and real time TDDFT (RT-TDDFT) has been employed to simulate the dynamic processes of electronic systems.[19] RT-TDDFT simulates usually the real time dynamics of isolated electronic systems subjected to electromagnetic fields. In 1998, we reported our linear scaling $O(N)$ time-dependent Hartree−Fock (TDHF)[20] method for excited states. The key quantity is the reduced single-electron density matrix (RSDM), and the equation of motion for the RSDM is derived and integrated in the time domain to model the dynamics of the electronic systems. Because the RSDM is an $N \times N$ matrix, we need solve only $O(N^2)$ differential equations, and thus the computational time of the RT-TDHF[20,21] scales as $O(N^3)$. When the system is large enough, the RSDM becomes a sparse matrix, the corresponding computational time is $O(N)$ only. Consequently, the RT-TDHF can be applied to systems containing thousands of electrons. Subsequently we extended the $O(N)$ method to TDDFT and applied the resulting $O(N)$ TDDFT to study the excited state properties of polyacetylene, carbon nanotubes (CNTs), and water clusters.[22,23] As early as in 2002, we attempted to combine quantum chemistry and quantum dissipation theory by developing a formalism to simulate the dynamics of the electronic systems subjected to phonon baths.[24] We start from the RT-TDHF method and write down the corresponding equation of motion for the RSDM. By assuming that the phonon bath is in thermal equilibrium, we integrate out the phonon degrees of freedom and derive the closed equation of motion for the RSDM. In the resulting formalism, the energy of the system is not conserved as the electrons and phonons exchange energy. However, there is no exchange of electrons with the external bath and thus the system is still a closed system. As the RSDM is an $N \times N$ matrix, the corresponding computational time of the RSDM-based RT-TDHF scales as $O(N^3)$ and is much less expensive than the conventional QDT, which is based on the equation of motion for the RDM [an $O(M! \times M!)$ matrix]. As a result, the RSDM-based RT-TDHF method was employed to simulate successfully the photoexcitation and subsequent nonradiative decay of a butadiene molecule. Recently, there are also works that apply TDDFT for a canonical open system to study thermalized electronic systems.[25,26] Based on our earlier work in 2002,[24] we conjectured that combining RT-TDDFT and NEGF may lead to a generalized TDDFT for open electronic systems. The key quantity would be the RSDM and the key equation is thus the equation of motion of the RSDM.

In 2007, we reported our work extending RT-TDDFT to simulate open electronic systems by combining TDDFT and NEGF. The resulting TDDFT-OS is based on the equation of motion for the RSDM of the system of interests, and its computational time scales as $O(N^3)$. Moreover, the number of electrons in the system of interests is not conserved and often fractional. For the first time, the real time simulation of the realistic molecular electronic device was carried out from first-principles quantum mechanics.[17]

There are also other research teams working on the implementation of TDDFT for open systems, and their approaches include solving the double time-integral Dyson equation,[27] Green's function,[28] the Kadanoff−Baym equations,[29,30] and the Kohn−Sham Master Equation.[31,32] In this Account, we outline the theoretical foundation of the TDDFT-OS theory, the resulting equation of motion for RSDM, and its numerical implementation and review the subsequent applications in molecular electronics[33,34] and scanning tunneling microscopy (STM).[35]

2. THEORY

2.1. Theoretical Foundation: Holographic Electron Density Theorem

The theoretical foundation for DFT lies in Hohenberg−Kohn theorem,[36] which states that the ground state electron-density function determines uniquely the external potential and thus all electronic properties of the system. Similarly, TDDFT is based on Runge−Gross theorem,[18] which shows that time-dependent electron density $\rho(\vec{r},t)$ determines the electronic properties of a time-dependent system. To apply TDDFT to an open system, we ask whether the electron density in a subsystem of interest can determine the electron density of the entire system and thus the physical properties of the subsystem of interest. It turns out for real physical systems made of atoms and molecules, the electron density of any eigenstates (including the ground state) is a real analytic quantity. This is known as the holographic electron density theorem (HEDT), first conjectured by Riess and Münch[37] and proved by Fournais et al.[38,39] The analyticity of electron density means that given a piece of electron density on a finite subspace, we can in principle perform analytical continuation to determine the electron density of the rest of the entire system and thus further determine the external potential and electronic properties of the entire system according to Hohenberg and Kohn theorem.

HEDT can be extended to the time-dependent case.[17] If the initial electron density $\rho(\vec{r},\ t\ =\ 0)$ and the time-dependent external potential $\nu(\vec{r},\ t)$ are real analytic quantities in real space, then the electron density on any finite subsystem at any time $\rho_D(\vec{r},\ t)$ has one-to-one correspondence with $\nu(\vec{r},\ t)$ of the entire system and determines uniquely the electron density of the entire system. Therefore, in principle, we can extract all electronic properties of the system from the electron density of the subsystem of interest, which is the open electronic system that we are interested in. This time-dependent holographic electron density theorem (TD-HEDT) provides the theoretical foundation to apply TDDFT for open system. TDDFT-OS may be extended to include the current density as an additional basic variable, just as is included as the basic physical quantity of interest, the stochastic time-dependent current-density functional theory (TDCDFT).[40]

2.2. Formulation: TDDFT for an Open System

Figure 1 shows a typical open electronic system, in which the central region D is coupled to two electrodes L and R. Region D is the open system of our interest while regions L and R are often of macroscopic sizes and treated as the environment.

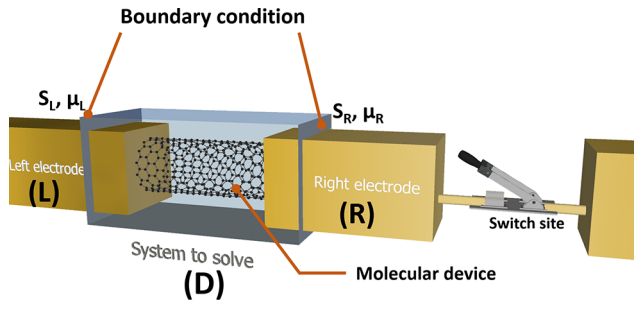

Figure 1. Schematic diagram showing a molecular junction.

DOI: 10.1021/acs.accounts.7b00382
Acc. Chem. Res. 2018, 51, 385−393

The Liouville−von Neumann equation for the RSDM, σ_D, of the open system can be written as

$$i\frac{d}{dt}\boldsymbol{\sigma}_D(t) = [\mathbf{h}_D(t), \boldsymbol{\sigma}_D(t)] - i\sum_{\alpha=L,R}\mathbf{Q}_\alpha(t) \quad (1)$$

where $\mathbf{h}_D(t)$ is the KS Fock matrix of the device region D and $\mathbf{Q}_\alpha(t)$ is the dissipative term, which characterizes the dissipative interactions, including the exchange of electrons and energy between the device region D and environment α. Its trace gives time-dependent electric current passing from environment α into the device region.

$$J_\alpha(t) = -eTr[\mathbf{Q}_\alpha(t)] \quad (2)$$

Equation 1 is in principle a closed equation of motion for RSDM since $\mathbf{h}_D(t)$ and $\mathbf{Q}_\alpha(t)$ are both functionals of electron density in the device region according to TD-HEDT. In practice, we can follow the NEGF formalism to evaluate $\mathbf{Q}_\alpha(t)$. To track $\mathbf{Q}_\alpha(t)$ in time, we introduce the dissipation matrices whose dynamics can be solved via the additional sets of equations of motion (EOM), which are elaborated in next section.

The procedures for simulating time-dependent open systems are summarized as a flowchart in Figure 2. First, the initial state of our system of interest needs to be determined. We assume that at $t = 0$, the system is in equilibrium with its environment. In this case, we can apply DFT-NEGF method[15,16] to obtain self-consistently the equilibrium KS Fock matrix $\mathbf{h}_D(0)$ and the equilibrium density $\rho_D(\vec{r}, 0)$. Once $\mathbf{h}_D(0)$ is known, the initial values of the RSDM and dissipation matrices can be constructed. Next, we propagate the EOM while updating the KS Hamiltonian for every time step. The change of the KS Hamiltonian induced by bias voltage has two terms, namely, the Hartree and XC components.

$$\mathbf{h}_D(t) = \mathbf{h}_D(0) + \delta\mathbf{V}_H(t) + \delta\mathbf{V}_{XC}(t) \quad (3)$$

The change in XC potential $\delta\mathbf{V}_{XC}(r, t)$ is updated according to the change of the electron density $\delta\rho(r, t)$. The exchange-correlation potential $\delta\mathbf{V}_{XC}[\delta\rho(r, t)]$ is in principle nonlocal in both space and time. In practice, we employ adiabatic approximation such that the time-dependence is local.

Induced Hartree potential $\delta V_H(r, t)$ is solved via the Poisson equation,

$$\nabla^2\delta V_H(r, t) = -4\pi\delta\rho(r, t) \quad (4)$$

which is subjected to the boundary conditions,

$$\delta V_H(r, t)|_{S_L} = \Delta_L(t) \quad (5)$$

$$\delta V_H(r, t)|_{S_R} = \Delta_R(t) \quad (6)$$

where S_L and S_R denote the interfaces between the device and the electrodes L/R (as indicated in Figure 1). $\Delta_{L/R}(t)$ are the bias voltages applied on them.

2.3. Numerical Schemes

In this section, we discuss three numerical implementation schemes. The first one is the Lorentzian−Padé decomposition scheme,[41−43] which approximates the self-energy of the electrodes and Fermi−Dirac distribution via Lorentzian and Padé expansions, respectively. The second one is the Chebyshev decomposition scheme,[44] which is very accurate and applicable to both finite and zero temperature. However, it can be computationally expensive since the number of expansion terms is proportional to the simulation time. The last scheme is the wide band limit (WBL) approximation,[45] which neglects the energy-dependence of electrodes' self-energies. This approximation greatly simplifies the EOM and therefore allows simulations of larger systems. We describe briefly the three schemes below.

2.3.1. Lorentzian−Padé Decomposition Scheme. The Lorentzian−Padé decomposition scheme involves approximating the line-width function, $\mathbf{\Lambda}_\alpha(E)$, by a summation of Lorentzian functions and the Fermi−Dirac distribution by Padé spectrum decomposition:[46]

$$\mathbf{\Lambda}_\alpha(\varepsilon) \approx \sum_{d=1}^{N_d}\frac{w_d^2}{(\varepsilon - \Omega_d)^2 + w_d^2}\bar{\mathbf{\Lambda}}_{\alpha,d} \quad (7)$$

$$f(\varepsilon - \mu_\alpha) \approx \frac{1}{2} - \sum_{p=1}^{N_p}\left(\frac{R_p}{\varepsilon - \mu_\alpha + iz_p} + \frac{R_p}{\varepsilon - \mu_\alpha - iz_p}\right) \quad (8)$$

Practically, the Lorentzian approximation can be obtained by least-squares fitting of the self-energies[42] or evaluating the self-energies with complex absorbing potential.[43] The number of Padé expansion, N_p, is chosen such that the error of the approximated Fermi−Dirac function within the bandwidth of the system is less than a given tolerance. With these two approximations, the following closed set of EOM can be derived.

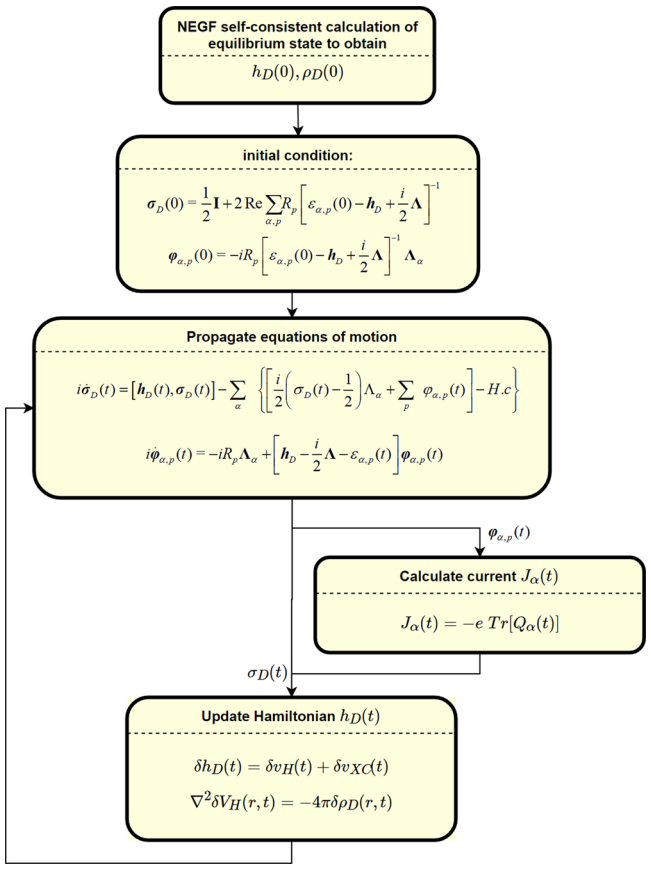

Figure 2. Flowchart for a TDDFT-OS calculation (under WBL approximation).

DOI: 10.1021/acs.accounts.7b00382
Acc. Chem. Res. 2018, 51, 385−393

$$i\dot{\boldsymbol{\sigma}}_{\mathrm{D}}(t) = [\mathbf{h}_{\mathrm{D}}(t), \boldsymbol{\sigma}_{\mathrm{D}}(t)] - \sum_{\alpha,k} (\boldsymbol{\varphi}_{\alpha,k}(t) - \boldsymbol{\varphi}_{\alpha,k}^{\dagger}(t)) \tag{9}$$

$$i\dot{\boldsymbol{\varphi}}_{\alpha,k}(t) = [\mathbf{h}_{\mathrm{D}}(t) - \varepsilon_{\alpha,k}(t)]\boldsymbol{\varphi}_{\alpha,k}(t) - [i\mathbf{A}_{\alpha,k}^{<} + \boldsymbol{\sigma}_{\mathrm{D}}\boldsymbol{\Lambda}_{\alpha,k}] + \sum_{\alpha'k'} \boldsymbol{\varphi}_{\alpha k,\alpha' k'}(t) \tag{10}$$

$$i\dot{\boldsymbol{\varphi}}_{\alpha k,\alpha' k'}(t) = [\varepsilon_{\alpha',k'}^{*}(t) - \varepsilon_{\alpha,k}(t)]\boldsymbol{\varphi}_{\alpha k,\alpha' k'}(t) + \boldsymbol{\Lambda}_{\alpha',k}\boldsymbol{\varphi}_{\alpha,k}(t) - \boldsymbol{\varphi}_{a',k'}^{\dagger}(t)\boldsymbol{\Lambda}_{\alpha,k} \tag{11}$$

where $\boldsymbol{\varphi}_{\alpha,k}(t)$ is the first tier dissipation matrix, resulting from the decomposition of the dissipative term, that is, $\mathbf{Q}_{\alpha}(t) = -i\sum_k[\boldsymbol{\varphi}_{\alpha,k}(t) - \boldsymbol{\varphi}_{\alpha,k}^{\dagger}(t)]$, and $\boldsymbol{\varphi}_{\alpha k,\alpha' k'}(t)$ is the second-tier dissipation matrix, which emerges from the EOM of $\boldsymbol{\varphi}_{\alpha,k}(t)$. Initial conditions of the RSDM and dissipation matrices can be constructed for the initial equilibrium.[41,42]

2.3.2. Chebyshev Decomposition Scheme. Since the KS Fock matrix of the electrode is bounded both from below and above, the spectral function of electrode, $A_{\alpha}(E)$, is only nonzero for a finite interval, let us say $[\bar{\omega} - \Omega, \bar{\omega} + \Omega]$. The key of the Chebyshev decomposition scheme[44] is to make use of the Jacobi–Anger identity to expand the time-dependent phase e^{iEt} into Chebyshev polynomials.

$$e^{i\Omega xt} = \sum_{n=1}^{M} (2 - \delta_{n,0}) i^n J_n(\Omega t) T_n(x) \tag{12}$$

where J_n is the Bessel function of the first kind of integer order and T_n is the Chebyshev polynomial of the first kind. It is noted that $|T_n(x)|$ is bounded by 1 within the interval $[-1,1]$ and $J_n(x)$ decays to zero spectrally as n increases for fixed x,

$$J_n(x) \approx \frac{1}{\sqrt{2\pi n}}\left(\frac{xe}{2n}\right)^n \quad \text{as} \quad n \to \infty \tag{13}$$

Therefore, given the simulation time $t_{\max}$ and Ω, we can truncate the series after M terms such that $J_{M+1}(\Omega t_{\max})$ is smaller than the desired tolerance.

After some algebraic manipulations, we can arrive at the following EOM:

$$i\dot{\boldsymbol{\sigma}}_{\mathrm{D}}(t) = [\mathbf{h}_{\mathrm{D}}(t), \boldsymbol{\sigma}_{\mathrm{D}}(t)] - \sum_{\alpha,n} [\Omega i^n J_n(\Omega(t - t_0))\boldsymbol{\varphi}_{\alpha,n}(t) - \mathrm{Hc}] \tag{14}$$

$$i\dot{\boldsymbol{\varphi}}_{\alpha,n}(t) = [\mathbf{h}_{\mathrm{D}}(t) - \bar{\omega} - \Delta_{\alpha}(t)]\boldsymbol{\varphi}_{\alpha,n}(t) + (2 - \delta_{n,0})[\boldsymbol{\Xi}_{\alpha,n}(t) - \boldsymbol{\sigma}_{\mathrm{D}}(t)\boldsymbol{\Pi}_{\alpha,n}(t)] + \sum_{\alpha' n'} (-i)^{n'}\Omega J_{n'}(\Omega(t - t_0))\boldsymbol{\varphi}_{\alpha n,\alpha' n'}(t) \tag{15}$$

$$i\dot{\boldsymbol{\varphi}}_{\alpha n,\alpha' n'}(t) = [\Delta_{\alpha'}(t) - \Delta_{\alpha}(t)]\boldsymbol{\varphi}_{\alpha n,\alpha' n'}(t) + (2 - \delta_{n',0})\boldsymbol{\Pi}_{\alpha' n'}^{*}(t)\boldsymbol{\varphi}_{\alpha,n}(t) - (2 - \delta_{n,0})\boldsymbol{\varphi}_{\alpha' n'}^{\dagger}(t)\boldsymbol{\Pi}_{\alpha,n}(t) \tag{16}$$

where

$$\boldsymbol{\Xi}_{\alpha,n} = \int_{-1}^{1} \mathrm{d}x T_n(x)\tilde{f}_{\alpha}(x)\tilde{\boldsymbol{\Lambda}}_{\alpha}(x) \tag{17}$$

$$\boldsymbol{\Pi}_{\alpha,n}(t) = \int_{-1}^{1} \mathrm{d}x T_n(x) e^{-i\Omega x(t-t_0)}\tilde{\boldsymbol{\Lambda}}_{\alpha}(x) \tag{18}$$

$\tilde{f}_{\alpha}(x) = f_{\alpha}(\Omega x + \bar{\omega})$ and $\tilde{\Lambda}_{\alpha}(x) = \Lambda_{\alpha}(\Omega x + \bar{\omega})$ are the rescaled Fermi–Dirac function and spectral function.

2.3.3. Wide Band Limit Approximation. The WBL approximation assumes the the electrodes have infinitely large band widths and energy-independent broadening, that is, $\boldsymbol{\Lambda}_{\alpha}(\varepsilon) \approx \boldsymbol{\Lambda}_{\alpha}$. In practice, $\boldsymbol{\Lambda}_{\alpha}$ is usually the line width matrix evaluated at Fermi energy μ of the unbiased equilibrium system because electrons near Fermi energy are responsible for transport phenomenon and it gives correct steady state current at small bias limit. And the Fermi–Dirac distribution is again expanded by Padé decomposition. The resulting EOM are written as

$$i\dot{\boldsymbol{\sigma}}_{\mathrm{D}}(t) = [\mathbf{h}_{\mathrm{D}}(t), \boldsymbol{\sigma}_{\mathrm{D}}(t)] - \sum_{\alpha}\left\{\left[\frac{i}{2}\left(\boldsymbol{\sigma}_{\mathrm{D}}(t) - \frac{1}{2}\right)\boldsymbol{\Lambda}_{\alpha} + \sum_{p=1}^{N_p}\boldsymbol{\varphi}_{\alpha,p}(t)\right] - \mathrm{Hc}\right\} \tag{19}$$

$$i\dot{\boldsymbol{\varphi}}_{\alpha,p}(t) = -iR_p\boldsymbol{\Lambda}_{\alpha} + \left[\mathbf{h}_{\mathrm{D}} - \frac{i}{2}\boldsymbol{\Lambda} - \varepsilon_{\alpha,p}(t)\right]\boldsymbol{\varphi}_{\alpha,p}(t) \tag{20}$$

where $\varepsilon_{\alpha,p}(t) = \mu_{\alpha} + \Delta_{\alpha}(t) + iz_p$ and $\boldsymbol{\Lambda} = \sum_{\alpha}\boldsymbol{\Lambda}_{\alpha}$. We can see the EOM are closed without the need to introduce second-tier dissipation matrices. Therefore, the WBL scheme is much less computationally expensive compared to the previous two schemes.

The initial values of σ_{D} and $\varphi_{\alpha,p}$ can be evaluated by

$$\boldsymbol{\sigma}_{\mathrm{D}}(0) = \frac{1}{2}\mathbf{I} + 2\mathrm{Re}\sum_{\alpha,p} R_p\left[\varepsilon_{\alpha,p}(0) - \mathbf{h}_{\mathrm{D}} + \frac{i}{2}\boldsymbol{\Lambda}\right]^{-1} \tag{21}$$

$$\boldsymbol{\varphi}_{\alpha,p}(0) = -iR_p\left[\varepsilon_{\alpha,p}(0) - \mathbf{h}_{\mathrm{D}} + \frac{i}{2}\boldsymbol{\Lambda}\right]^{-1}\boldsymbol{\Lambda}_{\alpha} \tag{22}$$

2.4. Electron–Phonon Interaction

Inelastic scattering and energy dissipation due to electron–phonon interaction (EPI) can play important roles in charge transport and transfer, for instance, phonon-mediated charge transfer and local heating. The effects of EPI in molecular electronics have attracted extensive attention both experimentally and theoretically. But most studies focus on steady state properties, while transient effects are also important. Our EOM approach can be extended to take into account EPI by including the corresponding self-energies. In the weak EPI regime, the lowest order expansion (LOE) is employed.[47] In the strong EPI regime, the polaron transformation can be used.[48]

For the LOE, we expand the EPI dressed Green's function to the lowest order with respect to electron–phonon coupling matrix, γ_q, starting from the bare electron Green's function $\mathbf{G}_0(t,t')$.

$$\mathbf{G}^r(t, t') = \mathbf{G}_0^r(t, t') + [\mathbf{G}_0^r\boldsymbol{\Sigma}_{\mathrm{ep}}^r\mathbf{G}_0^r](t, t') \tag{23}$$

Furthermore, since the characteristic time scale of electronic processes is much smaller than that of phonon processes, the phonon is assumed to be in equilibrium and unperturbated by the electron. Under these two approximations, the EPI self-energy becomes

DOI: 10.1021/acs.accounts.7b00382
Acc. Chem. Res. 2018, 51, 385–393

$$\Sigma^{<}_{ep}(t, t') = \sum_{q,\pm} \gamma_q N_q^{\pm} e^{\pm i\omega_q(t-t')} \mathbf{G}_0^{<}(t, t')\gamma_q \tag{24}$$

where $N_q^{\pm} = N_q + \frac{1}{2} \pm \frac{1}{2}$. ω_q and N_q are the phonon frequency and occupation number (following the Bose−Einstein distribution) of the phonon mode q. This is also known as the extreme damping limit where heating of the phonon system is ignored. If nonequilibrium heating of the phonon system is considered, the number of phonons, N_q, has to be time dependent. One way to include it is to give a rate equation for N_q, including an external damping rate of phonons.

With the EPI self-energy, the dissipative term now contains two parts. One is $\mathbf{Q}_{L/R}(t)$, which is responsible for the electron exchange between the device and electrodes. Another one is $\mathbf{Q}_{ep}(t)$ responsible for inelastic scattering and energy dissipation of electrons due to EPI, Since EPI does not cause any particle dissipation, $\mathrm{Tr}[\mathbf{Q}_{ep}(t)]$ should be zero in order to ensure the current continuity.

We assume WBL approximation and Padé decomposition of the Fermi−Dirac function. And for simplicity, we will use bold letter $\mathbf{a}$ to denote the index pair (α, p), where α = L, R and p corresponds to the Padé terms, and $\mathbf{q}$ to denote (q, x) in the subscript, where q corresponds to each phonon mode and $x = \pm$.

The EOM under WBL approximation with EPI are

$$i\dot{\boldsymbol{\sigma}}_D(t) = [\mathbf{h}_D(t), \boldsymbol{\sigma}_D(t)] - i \sum_{\alpha=L,R,ep} \mathbf{Q}_\alpha(t) \tag{25}$$

$$i\dot{\boldsymbol{\varphi}}_{\mathbf{a}}(t) = -iR_p\boldsymbol{\Lambda}_\alpha + \left[\mathbf{h}_D - \frac{i}{2}\boldsymbol{\Lambda} - \varepsilon_{\alpha,p}(t)\right]\boldsymbol{\varphi}_{\mathbf{a}}(t) + \sum_{q,x} \boldsymbol{\gamma}_q \boldsymbol{\varphi}_{\mathbf{a},\mathbf{q}}(t) \tag{26}$$

$$i\dot{\boldsymbol{\varphi}}_{\mathbf{a},\mathbf{q}}(t) = -[\mathbf{G}^r(\varepsilon_{\alpha,p}(t) + x\omega_q)]^{-1}\boldsymbol{\varphi}_{\mathbf{a},\mathbf{q}}(t) + [N_q^{-x} + x\boldsymbol{\sigma}^0(t)]\boldsymbol{\gamma}_q\boldsymbol{\varphi}_{\mathbf{a}}^0(t) - x\sum_{a'} \boldsymbol{\varphi}_{\mathbf{a}',\mathbf{a},\mathbf{q}}(t) \tag{27}$$

$$i\dot{\boldsymbol{\varphi}}_{\mathbf{a}',\mathbf{a},\mathbf{q}}(t) = [\varepsilon^*_{\alpha',p'}(t) - x\omega_q - \varepsilon_{\alpha,p}(t)]\boldsymbol{\varphi}_{\mathbf{a}',\mathbf{a},\mathbf{q}}(t) - \boldsymbol{\varphi}_{\mathbf{a}'}^{\mathbf{0}\dagger}(t)\boldsymbol{\gamma}_q\boldsymbol{\varphi}_{\mathbf{a}}^{\mathbf{0}}(t) \tag{28}$$

We can see that the first-tier dissipation matrices $\boldsymbol{\varphi}_{\mathbf{a}}(t)$, dressed by EPI, now have an additional term, $\sum_{q,x}\boldsymbol{\gamma}_q\boldsymbol{\varphi}_{\mathbf{a},\mathbf{q}}(t)$, in their EOM. This introduces the second-tier and third-tier EPI dissipation matrices, $\boldsymbol{\varphi}_{\mathbf{a},\mathbf{q}}(t)$ and $\boldsymbol{\varphi}_{\mathbf{a}'\mathbf{a},\mathbf{q}}(t)$, respectively. $\boldsymbol{\sigma}^0(t)$ and $\boldsymbol{\varphi}_{\mathbf{a}}^0(t)$ are the RSDM and first tier auxiliary matrices undressed by EPI. They follow the EOM 19 and 20, respectively.

Finally, the EPI dissipation term $\mathbf{Q}_{ep}(t)$ can be decomposed into auxiliary matrices corresponding to each phonon mode, $\mathbf{Q}_{ep}(t) = -i\sum_{q,x}[\boldsymbol{\varphi}_{\mathbf{q}}(t)\boldsymbol{\gamma}_q - \mathrm{Hc}]$. The EOM of these auxiliary matrices are

$$i\dot{\boldsymbol{\varphi}}_{\mathbf{a},\mathbf{q}}(t) = [\mathrm{L} - x\omega_q]\boldsymbol{\varphi}_q(t) + \sum_a [\boldsymbol{\varphi}^{\dagger}_{a,\bar{q}}(t) - \boldsymbol{\varphi}_{a,q}(t)] - [N_q^x\boldsymbol{\sigma}^0(t)\boldsymbol{\gamma}_q\bar{\boldsymbol{\sigma}}^0(t) - N_q^x\bar{\boldsymbol{\sigma}}^0(t)\boldsymbol{\gamma}_q\boldsymbol{\sigma}0(t)] \tag{29}$$

where $\bar{\boldsymbol{\sigma}}^0 = 1 - \boldsymbol{\sigma}^0$, $\mathbf{q} = (q, -x)$ and Liouville operator $\mathbf{L}$ is defined as $\mathbf{LA} = [\mathbf{h}(0) - i\boldsymbol{\Lambda}]\mathbf{A} - \mathbf{A}[\mathbf{h}(0) + i\boldsymbol{\Lambda}]$.

3. APPLICATIONS

3.1. Time-Dependent Quantum Interference in Meta-Linked Benzene System

We have studied the quantum interference (QI) in the meta-linked benzene system. When a ring component is included in molecular circuits, QI may occur due to the multiple charge transport pathways. As shown in Figure 3, the way in which the ring is connected determines the conducting feature of the molecular device. For example, a para-linked benzene molecule with two equal pathways induces constructive QI and reinforces the current through the molecule. By contrast, a meta-linked benzene ring has two pathways with a π phase difference, which forbids the current from passing through the molecule. Many related works have been done in the past decade to investigate the QI in steady state,[49−51] while the dynamical features of QI in time domain have rarely been addressed. Moreover, theoretical studies suggest that QI may be utilized to construct molecular quantum interference effect transistors (QuIETs). However, its practicability depends on the survivability of the quantum interference under real conditions such as nuclear vibration. In this section, by employing the TDDFT-OS method, we explore two questions: (1) How does QI arise and develop with time? (2) How robust is the QI against nuclear vibration?

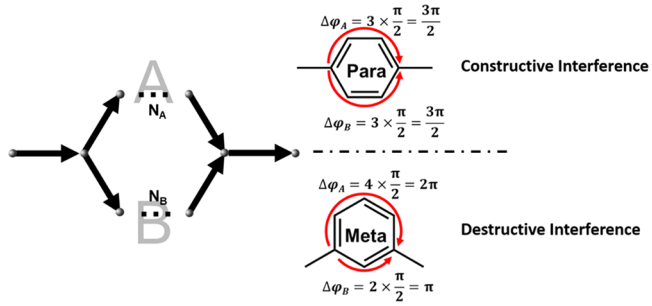

Figure 3. Quantum interference in molecules with multiple charge transport ways.

To figure out how quantum interference forms and evolves in time domain, we apply the TDDFT-OS method to a molecular strand with a linear chain of carbons either alone or enclosing a benzene ring, in the para or meta configuration. The systems are described by tight-binding models with 2 eV hoppings. The bias voltage is set as 0.01 V and is applied instantaneously at the initial time.

The simulation results are shown in Figure 4. In all three cases, we observe linearly increasing currents with respect to time at the beginning, which is consistent with our earlier work.[52] At time τ, the currents for para- and meta-linked benzene systems start to deviate from linear increase, where τ is exactly the time for electrons to travel at the Fermi velocity from the benzene ring to the left end (from site 1 to site 5) where the measurement takes place. After τ, the electrons from the ring reach the end of the molecular strand and the constructive and destructive interferences kick in, which result in the deviation of the currents and the difference in steady state values. The most important information drawn from the simulations is that QI requires time to develop rather than establishes instantaneously.

Having learned how QI develops in time domain, we turn to the topic of the robustness of QI against nuclear vibrations.

DOI: 10.1021/acs.accounts.7b00382
Acc. Chem. Res. 2018, 51, 385−393

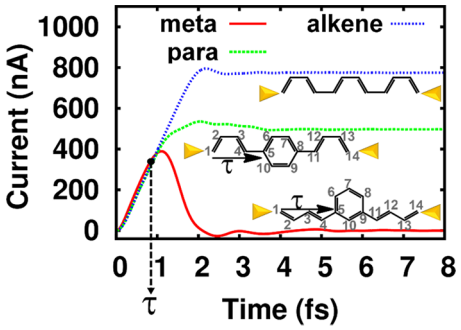

Figure 4. Time-dependent currents through the left electrodes of the meta, para, and alkene systems. The device region contains 14 carbon atoms for meta or para, and 12 carbon atoms for the single chain alkene. Reprinted with permission from ref 33. Copyright 2014 American Chemical Society.

Density functional tight-binding (DFTB) calculations are carried out on a benzene molecule attached to two semi-infinite extended alkene chains of equal bond lengths through the meta positions. The 10 atoms in the benzene ring are set to be movable, which is a reasonable simplification since it covers the two complete paths needed for the destructive QI. Bias voltage is applied exponentially with respect to time with an amplitude of 0.1 V, that is, $V(t) = 0.1\ \mathrm{V}(1 - \mathrm{e}^{-t/a})$, where the time constant a is set to 0.5 fs. All phonon modes are included in the calculations except the one with the lowest frequency, whose characteristic motion time is much longer than that of the electrons and therefore would not affect the transport process of the latter.[53] Temperature is set as 300 K for both the electrons in the electrodes and the phonons in the device region.

Figure 5 shows the comparison between the time-dependent current with the inclusion of electron−phonon interaction at

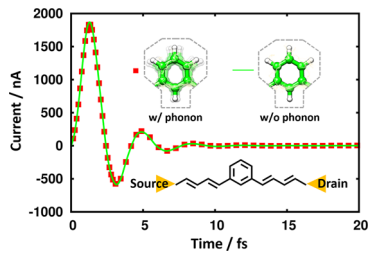

Figure 5. Comparison between the time-dependent currents through the electrodes of the meta-linked benzene molecule with and without phonon. The green solid line is the result without phonon; the red dots represent the result with phonons included at 300 K. Reprinted with permission from ref 34. Copyright 2017 American Chemical Society.

LOE level and the one in which the nuclei are fixed. The two current—time curves are aligned perfectly without any observable phase difference. More importantly, the times for the currents to reach their maximum values in the two methods are almost the same (∼1.3 fs). This is very crucial for the dynamics of the meta-linked benzene system, since it represents the time for charge carriers to travel at the Fermi velocity from the converging point of the two paths to the electrode where measurement takes place. In steady state calculations, the phonon self-energy is accounted for at both self-consistent Born approximation (SCBA) and LOE levels. The results suggest that the influence of the nuclear vibration on steady state current is insignificant. For example, the inclusion of electron−phonon interaction at LOE level only slightly enhances the steady current from 1.2 to 2.8 nA. As a comparison, under the same bias voltage, the steady state current of the para-linked benzene system is 6400 nA. Therefore, conclusion can be made that QI is robust against nuclear vibration not only in steady state but also in its transient dynamics, and thus the molecular quantum interference effect transistors can be realized.

3.2. Current-Induced Dissociation of Water Molecule on Metal Surface

Another application of the TDDFT-OS method is to study the current-induced single molecule chemical reaction under STM tips. Electrons injected from the STM tip can be used to control the formation or breaking of a chemical bond.[54] Few theoretical works were able to simulate such dynamics. TDDFT-OS coupled with Ehrenfest molecular dynamics (EhMD) can be employed to simulate such a problem. As a demonstration, we study the STM-induced dissociation of a water molecule. In simulation, the STM tip is placed over a water molecule on aluminum substrate with a separation of 5.5 Å. The geometry is optimized before a bias voltage of 4 V is applied.

From the simulation results, we observe a sudden surge in the time-dependent current measured at the STM tip, as shown in Figure 6. Such surge of current at ∼125 fs is associated with

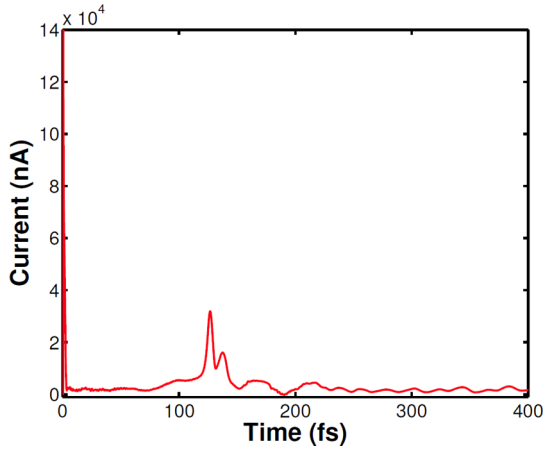

Figure 6. Time-dependent current measured at the STM tip. Reprinted with permission from ref 35. Copyright 2015 Zhang.

the breaking of chemical bond.[55] To confirm, we plot the snapshots of the structures along the EhMD trajectory in Figure 7, which suggests that the peak of the current around 125 fs in Figure 6 corresponds to the dissociation of a hydrogen atom from the water molecule. During the first 122 fs, the lengths of both the O−H and O−Al bond increase due to the electric field. After that, the H−O bond breaks, and the hydrogen atom flies off. Figure 8 shows the Mulliken charges of the two hydrogen atoms, where the hydrogen atom dissociated is labeled as H1 and the one remaining is labeled as H2. At the beginning, both the hydrogen atoms are positively charged due to the larger electronegativity of the oxygen atom. At ∼125 fs, the charge on H1 decreases rapidly from positive to negative, while it remains almost the same for H2. The increase in Coulomb repulsion between H1 and the oxygen atom leads to the dissociation of H1 atom. To confirm, we check the local density of states (LDOS) of the two hydrogen atoms at t = 120

DOI: 10.1021/acs.accounts.7b00382
Acc. Chem. Res. 2018, 51, 385−393

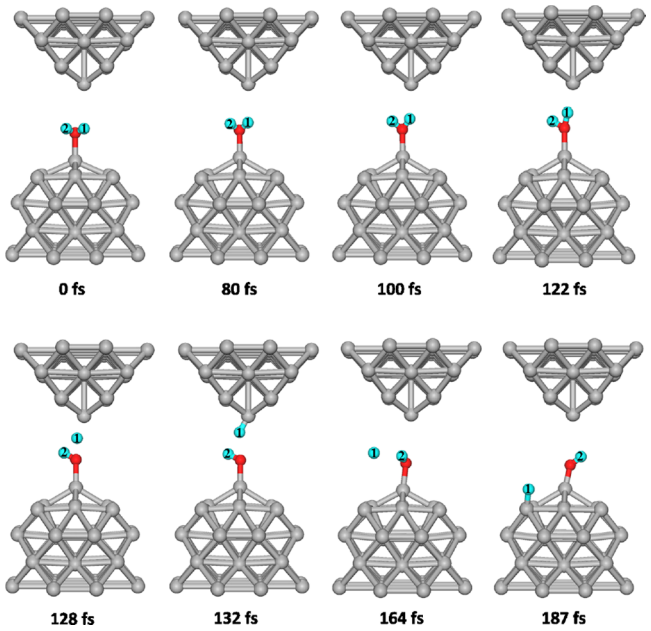

Figure 7. Current-induced decomposition of water molecule on metal surface. Reprinted with permission from ref 35. Copyright 2015 Zhang.

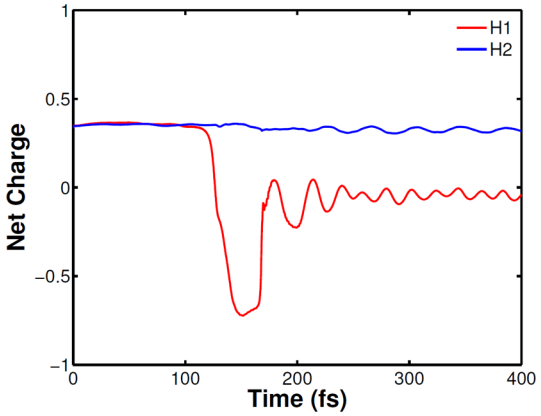

Figure 8. Mülliken charge of two hydrogen atoms. Reprinted with permission from ref 35. Copyright 2015 Zhang.

fs and find the unoccupied peaks of H1 above 4 eV when no bias voltage is applied. When a bias voltage larger than 4 eV is applied, these states enter the bias window and the Mülliken charge increases accordingly. By contrast, H2 has no LDOS in the bias window, and therefore its charge remains almost the same.

4. CONCLUSION AND OUTLOOK

TDDFT-OS combines the RT-TDDFT and NEGF formalisms and is applicable to simulate open electronic systems whose energy and number of electrons are not conserved. Efficient numerical algorithms have been developed to simulate realistic open systems and then applied to simulate the dynamics of molecular electronic devices and STM induced chemical reaction. TDDFT-OS can be further extended to include the effects of radiative decay by introducing a self-energy to account for the interaction between electromagnetic vacuum and electrons. It can be further extended to account for additional electron−electron correlation beyond the conventional exchange-correlation functionals, for instance, GW approximation.[56] The corresponding self-energy due to electron−electron interaction is a complex function whose real part is the usual correlation energy and the imaginary part corresponds to the inverse of the quasi-particle's lifetime due to electron−electron interaction. TDDFT-OS is well suited to simulate optoelectronic devices or processes by explicit or implicit inclusion of electromagnetic fields. Application of attosecond spectroscopy has led to sub-femtosecond resolution of electronic dynamics, and in particular, sub-nanometer spatial resolution if coupled to STM.[57] TDDFT-OS is perfect for modeling such experiments. Due to its complexity, the electrochemical process has eluded largely the attention of quantum chemists. An electrochemical cell is a typical open system and can be investigated with TDDFT-OS. The key challenge is the computational time as the dynamic processes of vast time scale differences are involved, electronic dynamics and ionic dynamics, and as such, further efforts are required to improve the computational efficiency of TDDFT-OS, which may be achieved via massive parallelization. Another important area of application of TDDFT-OS is quantum measurement theory. As TDDFT-OS is applicable to open systems containing thousands of electrons, it may be employed to simulate realistic measurement operations by including some portion of instrument as a part of open system of interest. A key issue in quantum computing is the coherence time of qubit. The longer the coherence time of qubit is, the more feasible the quantum computer is. This is another area where TDDFT-OS may be applicable.

AUTHOR INFORMATION

ORCID

GuanHua Chen: 0000-0001-5015-0902

Author Contributions

‡S.C. and Y.K. contributed equally to this work.

Notes

The authors declare no competing financial interest.

Biographies

Shuguang Chen received his B.Sc. and M.Phil. degree in Pharmacy from Peking University in 2007 and 2009, respectively. After that, he received his Ph.D. degree in theoretical chemistry in 2014 from The University of Hong Kong. His research interests are in quantum transport, molecular electronics, and excitation energy transfer in biological systems.

YanHo Kwok received his B.Sc. degree in Chemistry and Physics in 2011 and his Ph.D. degree in theoretical chemistry in 2016 from The University of Hong Kong. His research interests are in quantum dissipative systems, molecular electronics, and nolinear optical spectroscopy.

GuanHua Chen received his bachelor's degree in physics in 1986 from Fudan University and his Ph.D in physics from the California Institute of Technology in 1992. After postdoctoral training in University of Rochester, he joined the department of chemistry in The University of Hong Kong in 1996 and became a full Professor in 2006. Prof. Chen served as the Head of the Department of Chemistry during 2010−2016. He is also an honorary Professor in the department of Physics at HKU. His current research interests focus on first-principles methods for open systems, multiscale quantum mechanics/electromagnetics (QM/EM) method for device simulations, and application of machine learning in first-principles methods.

DOI: 10.1021/acs.accounts.7b00382
Acc. Chem. Res. 2018, 51, 385−393

■ ACKNOWLEDGMENTS

We thank the Research Grant Council of HKSAR (AoE/P-04/08, 17316016, HKU 700913P, HKU 700912P, HKUST9/CRF/11G), NFSC (21273186); HKU's Seed Fund for Strategic Research Theme for support.

■ REFERENCES

(1) Szabo, A.; Ostlund, N. S. *Modern Quantum Chemistry: Introduction to Advanced Electronic Structure theory*; Courier Corporation, 2012.
(2) Parr, R. G.; Weitao, Y. *Density-Functional Theory of Atoms and Molecules*; Oxford University Press, 1989.
(3) Kohn, W.; Sham, L. J. Self-Consistent Equations Including Exchange and Correlation Effects. *Phys. Rev.* **1965**, *140*, A1133−A1138.
(4) Yang, W. Direct calculation of electron density in density-functional theory. *Phys. Rev. Lett.* **1991**, *66*, 1438−1441.
(5) Weiss, U. *Quantum Dissipative Systems*; World Scientific, 2012.
(6) Redfield, A. G. The Theory of Relaxation Processes. *Adv. Magn. Opt. Reson.* **1965**, *1*, 1−32.
(7) Breuer, H. P.; Petruccione, F. *The Theory of Open Quantum Systems*; Oxford University Press, 2002.
(8) Lindblad, G. On the generators of quantum dynamical semigroups. *Commun. Math. Phys.* **1976**, *48*, 119−130.
(9) Fokker, A. D. Die mittlere Energie rotierender elektrischer Dipole im Strahlungsfeld. *Ann. Phys.* **1914**, *348*, 810−820.
(10) Planck, M. *Über einen Satz der statistischen Dynamik und seine Erweiterung in der Quantentheorie*; Reimer, 1917.
(11) Feynman, R. P.; Vernon, F. L. The Theory of a General Quantum System Interacting with a Linear Dissipative System. *Ann. Phys.* **2000**, *281*, 547−607.
(12) Caldeira, A. O.; Leggett, A. J. Influence of Dissipation on Quantum Tunneling in Macroscopic Systems. *Phys. Rev. Lett.* **1981**, *46*, 211−214.
(13) Tanimura, Y.; Kubo, R. Two-Time Correlation Functions of a System Coupled to a Heat Bath with a Gaussian-Markoffian Interaction. *J. Phys. Soc. Jpn.* **1989**, *58*, 1199−1206.
(14) Jin, J.; Zheng, X.; Yan, Y. Exact dynamics of dissipative electronic systems and quantum transport: Hierarchical equations of motion approach. *J. Chem. Phys.* **2008**, *128*, 234703.
(15) Xue, Y.; Datta, S.; Ratner, M. A. Charge transfer and "band lineup" in molecular electronic devices: A chemical and numerical interpretation. *J. Chem. Phys.* **2001**, *115*, 4292−4299.
(16) Taylor, J.; Guo, H.; Wang, J. Ab initio modeling of quantum transport properties of molecular electronic devices. *Phys. Rev. B: Condens. Matter Mater. Phys.* **2001**, *63*, 245407.
(17) Zheng, X.; Wang, F.; Yam, C. Y.; Mo, Y.; Chen, G. Time-dependent density-functional theory for open systems. *Phys. Rev. B: Condens. Matter Mater. Phys.* **2007**, *75*, 195127.
(18) Runge, E.; Gross, E. K. U. Density-Functional Theory for Time-Dependent Systems. *Phys. Rev. Lett.* **1984**, *52*, 997−1000.
(19) Yabana, K.; Bertsch, G. F. Time-dependent local-density approximation in real time. *Phys. Rev. B: Condens. Matter Mater. Phys.* **1996**, *54*, 4484−4487.
(20) Yokojima, S.; Chen, G. Time domain localized-density-matrix method. *Chem. Phys. Lett.* **1998**, *292*, 379−383.
(21) Yokojima, S.; Chen, G. Linear scaling calculation of excited-state properties of polyacetylene. *Phys. Rev. B: Condens. Matter Mater. Phys.* **1999**, *59*, 7259−7262.
(22) Yam, C. Y.; Yokojima, S.; Chen, G. Localized-density-matrix implementation of time-dependent density-functional theory. *J. Chem. Phys.* **2003**, *119*, 8794−8803.
(23) Yam, C.; Yokojima, S.; Chen, G. Linear-scaling time-dependent density-functional theory. *Phys. Rev. B: Condens. Matter Mater. Phys.* **2003**, *68*, 153105.
(24) Yokojima, S.; Chen, G. Excitation and dissipation of interacting many-electron system. *Chem. Phys. Lett.* **2002**, *355*, 400−404.
(25) Chapman, C. T.; Liang, W.; Li, X. Open-system electronic dynamics and thermalized electronic structure. *J. Chem. Phys.* **2011**, *134*, 024118.
(26) Nguyen, T. S.; Parkhill, J. Nonadiabatic Dynamics for Electrons at Second-Order: Real-Time TDDFT and OSCF2. *J. Chem. Theory Comput.* **2015**, *11*, 2918−2924.
(27) Ke, S.-H.; Liu, R.; Yang, W.; Baranger, H. U. Time-dependent transport through molecular junctions. *J. Chem. Phys.* **2010**, *132*, 234105.
(28) Stefanucci, G.; Almbladh, C. O. Time-dependent quantum transport: An exact formulation based on TDDFT. *EPL(Europhysics Letters)* **2004**, *67*, 14.
(29) Galperin, M.; Tretiak, S. Linear optical response of current-carrying molecular junction: A nonequilibrium Green's function−time-dependent density functional theory approach. *J. Chem. Phys.* **2008**, *128*, 124705.
(30) Myöhänen, P.; Stan, A.; Stefanucci, G.; van Leeuwen, R. Kadanoff-Baym approach to quantum transport through interacting nanoscale systems: From the transient to the steady-state regime. *Phys. Rev. B: Condens. Matter Mater. Phys.* **2009**, *80*, 115107.
(31) Yuen-Zhou, J.; Tempel, D. G.; Rodríguez-Rosario, C. A.; Aspuru-Guzik, A. Time-Dependent Density Functional Theory for Open Quantum Systems with Unitary Propagation. *Phys. Rev. Lett.* **2010**, *104*, 043001.
(32) Stefanucci, G.; Kurth, S.; Rubio, A.; Gross, E. K. U. Time-dependent approach to electron pumping in open quantum systems. *Phys. Rev. B: Condens. Matter Mater. Phys.* **2008**, *77*, 075339.
(33) Chen, S.; Zhang, Y.; Koo, S.; Tian, H.; Yam, C.; Chen, G.; Ratner, M. A. Interference and Molecular Transport—A Dynamical View: Time-Dependent Analysis of Disubstituted Benzenes. *J. Phys. Chem. Lett.* **2014**, *5*, 2748−2752.
(34) Chen, S.; Zhou, W.; Zhang, Q.; Kwok, Y.; Chen, G.; Ratner, M. A. Can Molecular Quantum Interference Effect Transistors Survive Vibration? *J. Phys. Chem. Lett.* **2017**, *8*, 5166−5170.
(35) Zhang, Q. Theory of Ehrenfest Dynamics for Open Systems and Its Applications, Postgraduate Thesis, The University of Hong Kong, 2015, DOI: 10.5353/th_b5699946.
(36) Hohenberg, P.; Kohn, W. Inhomogeneous Electron Gas. *Phys. Rev.* **1964**, *136*, B864.
(37) Riess, J.; Münch, W. The theorem of hohenberg and kohn for subdomains of a quantum system. *Theor. Chim. Acta* **1981**, *58*, 295−300.
(38) Fournais, S.; Hoffmann-Ostenhof, M.; Hoffmann-Ostenhof, T.; Østergaard Sørensen, T. The Electron Density is Smooth Away from the Nuclei. *Commun. Math. Phys.* **2002**, *228*, 401−415.
(39) Fournais, S.; Hoffmann-Ostenhof, M.; Hoffmann-Ostenhof, T.; Østergaard Sørensen, T. Analyticity of the density of electronic wavefunctions. *Arkiv för Matematik* **2004**, *42*, 87−106.
(40) Di Ventra, M.; D'Agosta, R. Stochastic Time-Dependent Current-Density-Functional Theory. *Phys. Rev. Lett.* **2007**, *98*, 226403.
(41) Kwok, Y. H.; Xie, H.; Yam, C. Y.; Zheng, X.; Chen, G. H. Time-dependent density functional theory quantum transport simulation in non-orthogonal basis. *J. Chem. Phys.* **2013**, *139*, 224111.
(42) Xie, H.; Jiang, F.; Tian, H.; Zheng, X.; Kwok, Y.; Chen, S.; Yam, C.; Yan, Y.; Chen, G. Time-dependent quantum transport: An efficient method based on Liouville-von-Neumann equation for single-electron density matrix. *J. Chem. Phys.* **2012**, *137*, 044113.
(43) Xie, H.; Kwok, Y.; Jiang, F.; Zheng, X.; Chen, G. Complex absorbing potential based Lorentzian fitting scheme and time dependent quantum transport. *J. Chem. Phys.* **2014**, *141*, 164122−164122.
(44) Tian, H.; Chen, G. H. An efficient solution of Liouville-von Neumann equation that is applicable to zero and finite temperatures. *J. Chem. Phys.* **2012**, *137*, 204114−204114.
(45) Zhang, Y.; Chen, S. G.; Chen, G. First-principles time-dependent quantum transport theory. *Phys. Rev. B: Condens. Matter Mater. Phys.* **2013**, *87*, 085110.

DOI: 10.1021/acs.accounts.7b00382
Acc. Chem. Res. 2018, 51, 385−393

(46) Hu, J.; Xu, R.-X.; Yan, Y. Communication: Padé spectrum decomposition of Fermi function and Bose function. *J. Chem. Phys.* **2010**, *133*, 101106−101106.
(47) Zhang, Y.; Yam, C. Y.; Chen, G. Dissipative time-dependent quantum transport theory. *J. Chem. Phys.* **2013**, *138*, 164121−164121.
(48) Zhang, Y.; Yam, C.; Chen, G. Dissipative time-dependent quantum transport theory: Quantum interference and phonon induced decoherence dynamics. *J. Chem. Phys.* **2015**, *142*, 164101−164101.
(49) Stafford, C. A.; Cardamone, D. M.; Mazumdar, S. The quantum interference effect transistor. *Nanotechnology* **2007**, *18*, 424014.
(50) Markussen, T.; Stadler, R.; Thygesen, K. S. The Relation between Structure and Quantum Interference in Single Molecule Junctions. *Nano Lett.* **2010**, *10*, 4260−4265.
(51) Solomon, G. C.; Herrmann, C.; Hansen, T.; Mujica, V.; Ratner, M. A. Exploring local currents in molecular junctions. *Nat. Chem.* **2010**, *2*, 223−228.
(52) Chen, S.; Xie, H.; Zhang, Y.; Cui, X.; Chen, G. Quantum transport through an array of quantum dots. *Nanoscale* **2013**, *5*, 169−173.
(53) Lindsay, S. M.; Ratner, M. A. Molecular Transport Junctions: Clearing Mists. *Adv. Mater.* **2007**, *19*, 23−31.
(54) Dujardin, G.; Walkup, R. E.; Avouris, P. Dissociation of Individual Molecules with Electrons from the Tip of a Scanning Tunneling Microscope. *Science* **1992**, *255*, 1232−1235.
(55) Lastapis, M.; Martin, M.; Riedel, D.; Hellner, L.; Comtet, G.; Dujardin, G. Picometer-Scale Electronic Control of Molecular Dynamics Inside a Single Molecule. *Science* **2005**, *308*, 1000−1003.
(56) Hedin, L. New Method for Calculating the One-Particle Green's Function with Application to the Electron-Gas Problem. *Phys. Rev.* **1965**, *139*, A796−A823.
(57) Cocker, T. L.; Peller, D.; Yu, P.; Repp, J.; Huber, R. Tracking the ultrafast motion of a single molecule by femtosecond orbital imaging. *Nature* **2016**, *539*, 263−267.

DOI: 10.1021/acs.accounts.7b00382
Acc. Chem. Res. 2018, 51, 385−393